Linköping University Post Print

Bending flexibility, kinking, and buckling characterization of ZnO nanorods/nanowires grown on different substrates by high and low temperature methods

Riaz Muhammad, Alimujiang Fulati, Lili Yang, O Nour, Magnus Willander and P Klason

N.B.: When citing this work, cite the original article.

Bending flexibility, kinking, and buckling characterization of ZnO nanorods/nanowires grown on different substrates by high and low temperature methods

M. Riaz,[1,a)] A. Fulati,[1] L. L. Yang,[1] O. Nur,[1] M. Willander,[1] and P. Klason[2]

[1]*Department of Science and Technology, Campus Norrköping, Linköping University, SE-601 74 Norrköping, Sweden*
[2]*Department of Physics, Göteborg University, SE-412 96 Göteborg, Sweden*

Nanomechanical tests of bending flexibility, kinking, and buckling failure characterization of vertically aligned single crystal ZnO nanorods/nanowires were performed quantitatively by nanoindentation technique. These nanostructures were grown by the vapor liquid solid (VLS) method, a relatively high temperature approach, and the aqueous chemical growth (ACG) method, a relatively low temperature approach on different substrates, including SiC and Si. The first critical load at the inflection point found for the ZnO nanorods/nanowires grown by ACG method was 105 μN on the SiC substrates and 114 μN on the Si substrates. The corresponding buckling energies calculated from the force-displacement curves were 3.15×10^{-12} and 2.337×10^{-12} J, respectively. Similarly, for the samples grown by the VLS method, the first critical load at the inflection point and the corresponding buckling energies were calculated from the force-displacement curves as 198 μN and 7.03×10^{-12} J on the SiC substrates, and 19 μN and 1.805×10^{-13} J on the Si substrates. Moreover, the critical buckling stress, strain, and strain energy were also calculated for all samples. The strain energy for all samples was much less than the corresponding buckling energy. This shows that our as-grown samples are elastic and flexible. The elasticity measurement was performed for all the samples before reaching the first critical and kinking inflection point, and we subsequently observed the bending flexibility, kinking, and buckling phenomena on the same nanorods/nanowires. We observed that the loading and unloading behaviors during the bending test of the as-grown samples were highly symmetrical, and also that the highest point on the bending curves and the first inflection and critical point were very close. ZnO nanorods/nanowires grown on SiC by the ACG method, and those grown by the VLS method on Si substrates, show a linear relation and high modulus of elasticity for the force and displacement up to the first inflection and critical point. The results also show that the elasticity of the ZnO single crystal is approximately linear up to the first inflection point, is independent of the growth method and is strongly dependent on the verticality on the surface of the substrates. In addition, the results show that after the first buckling point, the nanorods/nanowires have plasticity, and become more flexible to produce multiple kinks. © *2008 American Institute of Physics.*
[DOI: 10.1063/1.3018090]

I. INTRODUCTION

One-dimensional semiconductor nanowires/nanorods such as InP, GaN, and ZnO have attracted increasing interest for their potential applications in electronic, piezoelectric, and photonic nanodevices.[1–3] ZnO nanorods/nanowires are important semiconducting and piezoelectric material structures that have various applications in the field of optoelectronics,[4] biosensors,[5] resonators,[6] electric nanogenerators,[7] and nanolasers.[8] ZnO-based quasi-one-dimensional materials have received increasing attention due to their unique characteristics in future nanodevices as nanoscale interconnects and active components of optical electronic devices and nanoelectromechanical systems (NEMSs). The dependence of their mechanical properties on size plays an important role in their application in NEMS and micro-

mechanical systems, which has recently led to much attention.[9] In addition, ZnO has a direct band gap with band gap energy of 3.37 eV at room temperature and has a large excitonic binding energy of 60 meV. Nanostructures based on wide band gap semiconductors such as GaN, SiC, and ZnO are of particular interest because of their applications in short wavelength light emitting devices and field emission devices.[10,11] Among these, ZnO has some extra advantages over the other nanostructures. First, as mentioned above, it exhibits both semiconducting and piezoelectric properties that can form the basis for electromechanically coupled sensors and transducers. Second, ZnO can be grown in a variety of nanostructures such as nanorings, nanobows, platelet circular structures, and Y-shape split ribbons and crossed ribbons, which could be unique for many applications in nanotechnology.[12] Finally, ZnO nanostructures can be grown on a variety of substrates of crystalline as well as amorphous surfaces.

---

a)Author to whom correspondence should be addressed. Electronic mail: riaz.muhammad@itn.liu.se.

104, 104306-1

Mechanical characterization of these nanostructures is very important for the reliability and efficient operation of the piezoelectric nanodevices. Mechanical reliability includes strength, toughness, stiffness, hardness, and adhesion with the substrate. Stiffness and adhesion measurements give us the stability of the nanostructure. Stiffness of the structures is to be determined both geometrically and from a material point of view. Structure failure may be due to improper design, i.e., design failure, rather than material failure. Buckling and instability of vertical structures are considered as design failure.[13] At present, there exists a collection of research reports on the mechanical properties of ZnO nanorods in literature.[9,14–22] Young *et al.*,[19] Wen *et al.*,[20] and Riaz *et al.*[22] discussed the buckling characterization of ZnO nanorods by using the nanoindentation method. Young *et al.*[19] and Wen *et al.*[20] used the Euler model for the characterization of long vertical ZnO nanorods. Riaz *et al.*[22] used the Euler model as well as the J.B. Johnson model for the characterization of long and intermediate ZnO nanorods. Recently, we performed an analysis comparing the buckling characterization of ZnO nanorods with adhesion energy, and observed that the buckling and adhesion energies of the as-grown nanorods were very close, leading us to the conclusion that the nanorods were unstabilized at the substrates.[23] There has been little work on understanding the bending flexibility, kinking and buckling of the vertical ZnO nanorods/nanowires grown on different substrates, or on evaluating the substrate effects on the bending flexibility, kinking, and buckling failure from the growth methods of high and low temperature approaches point of views.

In this work, we performed nanoindentation experiments to analyze the bending flexibility, kinking, and buckling failure phenomena of vertical ZnO nanorods/nanowires grown by vapor liquid solid (VLS) and aqueous chemical growth (ACG) methods on different substrates, including SiC and Si. The characterization was done both for long and intermediate nanorods/nanowires using the Euler buckling model and the J.B. Johnson buckling model. We also calculated the critical load for a single nanorod/nanowire, and then calculated the modulus of elasticity, critical buckling stress, strain, and strain energy for each sample.

II. EXPERIMENTAL

The ZnO nanowires/nanorods used in the present experiment were grown on SiC and Si substrates by the ACG method and the VLS method. In the ACG method, zinc nitride dihydrate $[Zn(NO_3)_26H_2O]$ was mixed with hexamethylene-tetramine (HMT) $(C_6H_{12}N_4)$ using the same molar concentration for both solutions. The molar concentration was varied from 0.025 to 0.075M. The two solutions were stirred together and the substrates were placed inside the solution. Then, it was heated up to 90 °C for 3 h. Before the substrates were placed inside the solution, they were coated with a ZnO seed layer using the technique develop by Greene *et al.*[24] Zinc acetate dihydrate was diluted in ethanol to a concentration of 5 mM. Droplets of the solution were placed on the substrate until they completely covered the sample surface. After 10 s, the substrates were rinsed in eth-

anol and then dried in air. This procedure was repeated five times and then the samples were heated to 250 °C in air for 20 min to yield layers of ZnO on the substrates. The whole procedure was repeated twice in order to ensure a uniform ZnO seed layer. The side with the seed layer was mounted face down in the solution. After the growth was completed, the samples were cleaned in de-ionized water and left to dry in air inside a closed beaker.

In the VLS technique, ZnO powder (99.9%) was mixed with graphite powder in a weight ratio of 1:1. Typically, 50–70 mg of the mixed powder was placed in a ceramic boat and the boat was then placed inside a quartz glass tube. The substrates were coated with a thin metal layer functioning as a catalyst and placed on top of the powder. In this study, gold (Au) with a thickness of 1–5 nm was used as a metal catalyst. The side coated with Au was placed face down, toward the powder. The distance between the powder and the substrate was 3 mm. The growth temperature was varied between 890 and 910 °C and the growth time was varied between 30 and 90 min.

X-ray diffraction (XRD) experiments were done using Cu $K\alpha1$ (λ=1.5406 Å) to characterize the crystallographic properties of the as-grown ZnO nanorods/nanowires. Surface morphologies of the sample and the size distribution of the nanorods/nanowires were characterized by a LEO 1550 scanning electron microscope (SEM). The buckling failure phenomena and bending behavior of the nanorods/nanowires were investigated by means of a hysitron nanoindenter. The nanorods/nanowires were uniaxially compressed with a conical diamond tip indenter on fused quartz of 1 μm radius.

Figure 1 shows typical SEM images of the as-grown ZnO nanorods/nanowires grown by the ACG method. Figures 1(a) and 1(b) show top and side views of the ZnO nanorods/nanowires grown on the SiC substrate and Figs. 1(c) and 1(d) show the low and high magnification of ZnO nanowires grown on the Si substrate. As can be seen, the nanorods are hexagonally arranged on the substrate. The approximate diameter, length and density of the nanorods were determined to be about 120 ± 55 nm, 1724 ± 117 nm, and 3.8×10^9 cm^{-2} on the SiC substrates and 85.5 ± 22 nm, 287 ± 23 nm, and 2.87×10^9 cm^{-2} on the Si substrates, respectively. SEM analysis of the as-grown ZnO nanorods/nanowires grown by the VLS method on the SiC and Si substrates was also performed (not shown here) and the results showed that the approximate diameter, length, and density of the nanorods/nanowires were determined to be about 311 ± 126 nm, 1713 ± 193 nm, and 4.87×10^8 cm^{-2} on the SiC substrates and 50 ± 13 nm, 683 ± 88 nm, and 6.0×10^9 cm^{-2} on the on SiC and Si substrates, respectively. It was found that the ZnO nanorods were vertically aligned along the *c*-axis and distributed uniformly across the entire substrate. From the measured XRD spectra of the sample (not shown), we observed peaks in the spectra indicating that the (0002) plane of ZnO nanorods/nanowires is the dominating reflection. These XRD peaks show that our nanorods were epitaxially grown along the *a*-plane for all the substrates. In addition, the XRD peaks of the ZnO (0002) plane show that the nanorods were vertically grown in the *c*-axis direction with good crystal quality. Figures 2 and 3 show the
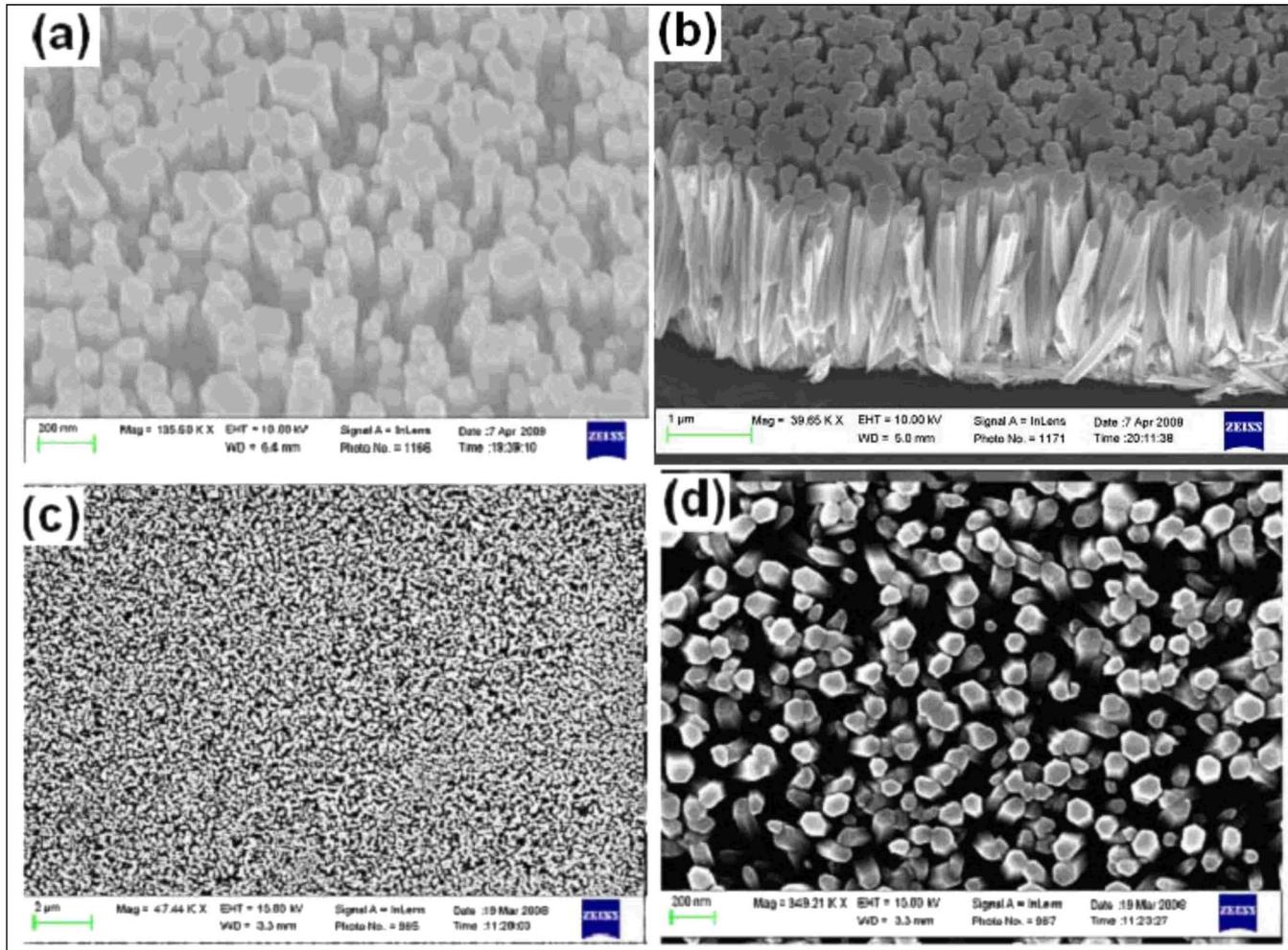
FIG. 1. (Color online) SEM images show the morphologies of the as-grown vertically aligned ZnO nanorod arrays. (a) and (b) show the top and side views grown on SiC substrate, (c) and (d) show nanowires grown on the Si substrate by the ACG method.

force versus displacement curves from nanoindentation experiments of the as-grown ZnO nanorods/nanowires by the ACG and VLS methods, respectively.

III. RESULTS AND DISCUSSION

Vertical ZnO nanorods/nanowires of 120 ± 55, 85.5 ± 22, 311 ± 126, and 50 ± 13 nm in diameter and 1724 ± 117, 287 ± 23, 1713 ± 193, and 683 ± 88 nm in length, respectively, were used in the nanoindentation experiment. The nanorods were loaded to a prescribed force and then unloaded in a force-controlled mode. Because each test was destructive in nature, several tests were conducted to check for repeatability. Figures 2(a), 2(c), 2(b), and 2(d) show the buckling and bending force-displacement curves for the as-grown samples by the ACG method. Similarly, Figs. 3(a), 3(c), 3(b), and 3(d) show the buckling and bending force-displacement curves for the as-grown samples by VLS method. The nanorods/nanowires grown by ACG method were observed to be unstable at a load of 105 and 114 μN on the SiC and Si substrates, respectively, while the samples grown by VLS method become unstable at a load of 198 μN for the former and 19 μN for the latter. The corresponding buckling energies were found to be 3.15×10^{-12}, 2.337×10^{-12}, 7.03

$\times 10^{-12}$, and 1.805×10^{-13} J, respectively. In all samples, the critical loads were found after the bending test. The main indication of buckling is deformations in the direction of the compressive load that suddenly change at a critical load into a transverse deformation, resulting in a sudden or catastrophic collapse of the nanorods. The change in the deformation direction is mainly due to the loss of verticality of the nanorods. In the loss of verticality, the nanorods/nanowires are either broken, produce other inflection and critical points, or deadhere from the substrate.

In Figs. 2(a), 2(c), 3(a), and 3(c), the loading portion consists of multiple zones, i.e., zone "0-1, 1-2, 2-3, 3-4, 4-5, 5-6, 6-7, and 7-8." In zone "0-1" of each curve, the data shows an initial increase with the displacement in which the nanorods are almost vertical and stable. This is the stable configuration as described schematically in Fig. 4(a). This linear rise is followed by a sharp change in displacement at essentially the same force and the curve becomes flat (i.e., zone "1-2"), which corresponds to a critical equilibrium configuration of the nanorods/nanowires. This is seen in Fig. 4(b). The force at this region is the first critical force on the nanorods/nanowires. A slight increase in the load will lead to instability and perturbation of the nanorods/nanowires shown in zone "2-3." This condition is described as in Fig. 4(c).
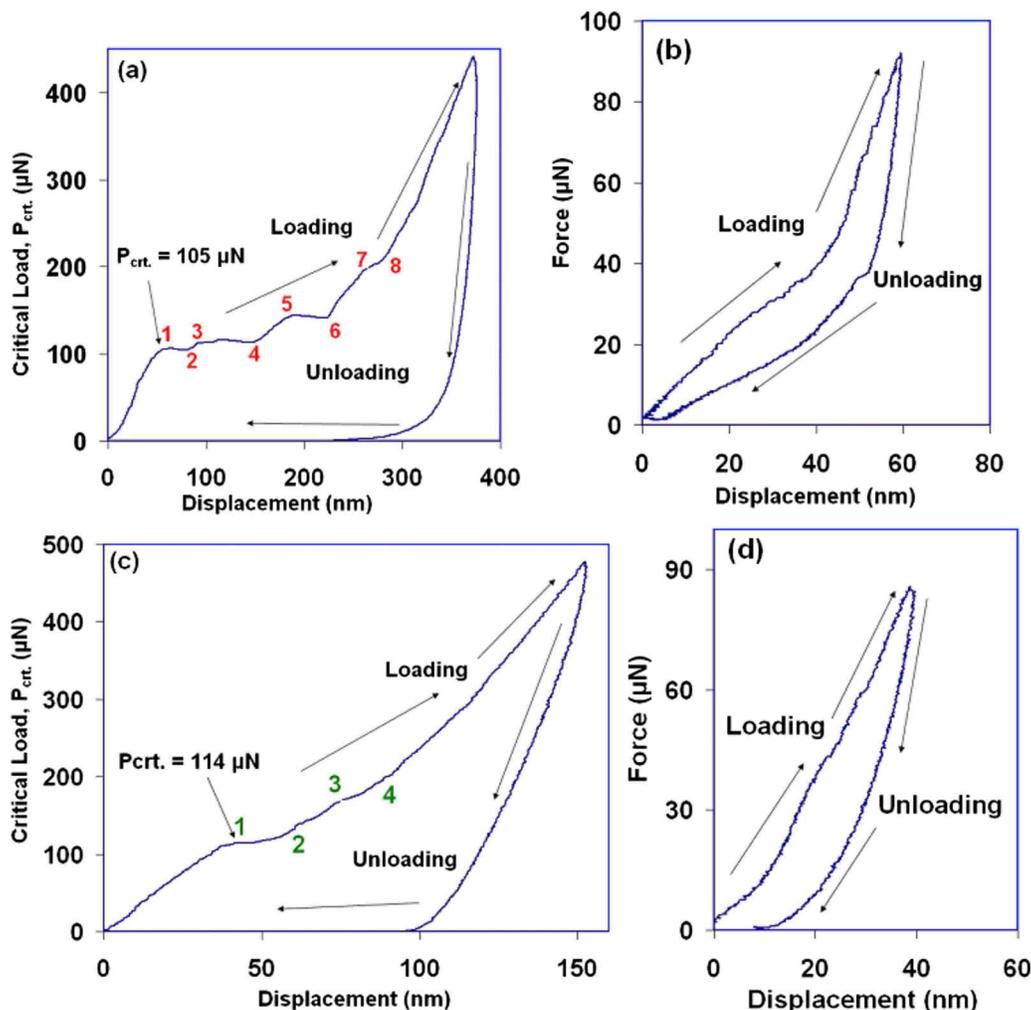
FIG. 2. (Color online) Load vs displacement curve of the as-grown ZnO nanorods/nanowires from nanoindentation experiments, where (a) and (c) show load displacement curves for kinking and buckling and (b) and (d) show the bending flexibility curves for the ZnO nanorods/nanowires grown by ACG method on SiC and Si substrates.

Other zones after the first inflection point of the loading portion show that the nanorods/nanowires lead into an alternative buckled configuration such as those shown in zones "2-3, 3-4, 4-5, 5-6, 6-7, and 7-8," where other critical and inflection points are developed for the preceding buckled configuration. Points 3, 5, and 7 are other multiple critical and inflection points of the as-grown samples. Usually after the first critical point 1, the nanorods/nanowires either break leading to the tip going into the substrate, or develop multiple buckling points leading to fracture. The alternative buckled configurations become strain hardened and larger force is required for buckling to occur. This strain hardening is due to the increase in dislocation density. Zones 2-3, 3-4, 4-5, 5-6, 6-7, and 7-8 show the force applied on the buckled configuration, in which the tip of the indenter had been exerting very large force as compared to zone 0-1. We are only interested in the first critical load in which the straight prebuckling configuration of the nanorods ceased. The instability and buckling characterization presented in this work is loss of the verticality of the ZnO nanorods under compressive overstresses.

In bending, the nanorods/nanowires were axially compressed by the nanoindentor tip in a controlled load mode

and then unloaded in the same way in equal intervals of time. Figures 2(b), 2(d), 3(b), and 3(d) show, for the bending, that the loading and unloading behavior is highly symmetrical. During the bending tests, we did not observe the buckling critical points of the nanorods/nanowires. After bending, exactly on the same area of nanorods/nanowires the load was increased to achieve the first and other buckled critical points for the as-grown samples. The top of the bending curves and the first critical points are very close to each other, showing that all the samples have a linear elasticity up to the first failure point. The nanorods/nanowires grown by the VLS method on the Si substrate exhibit a highly linear relation between the force and displacement as compared to all other samples. This may be because on the Si substrates, the nanorods/nanowires are relatively small in size and equal in length. In addition, the density of the nanowires is greater than the other samples, so more nanowires were under the tip. All of these factors provide a good relation between the force and displacement. The second reason may be that the nanowires are more vertical and of better quality than the other samples. In continuum mechanics, buckling is a nonlinear structural phenomenon,[25] whereas our experiments show that the behavior of all the as-grown samples is ap-
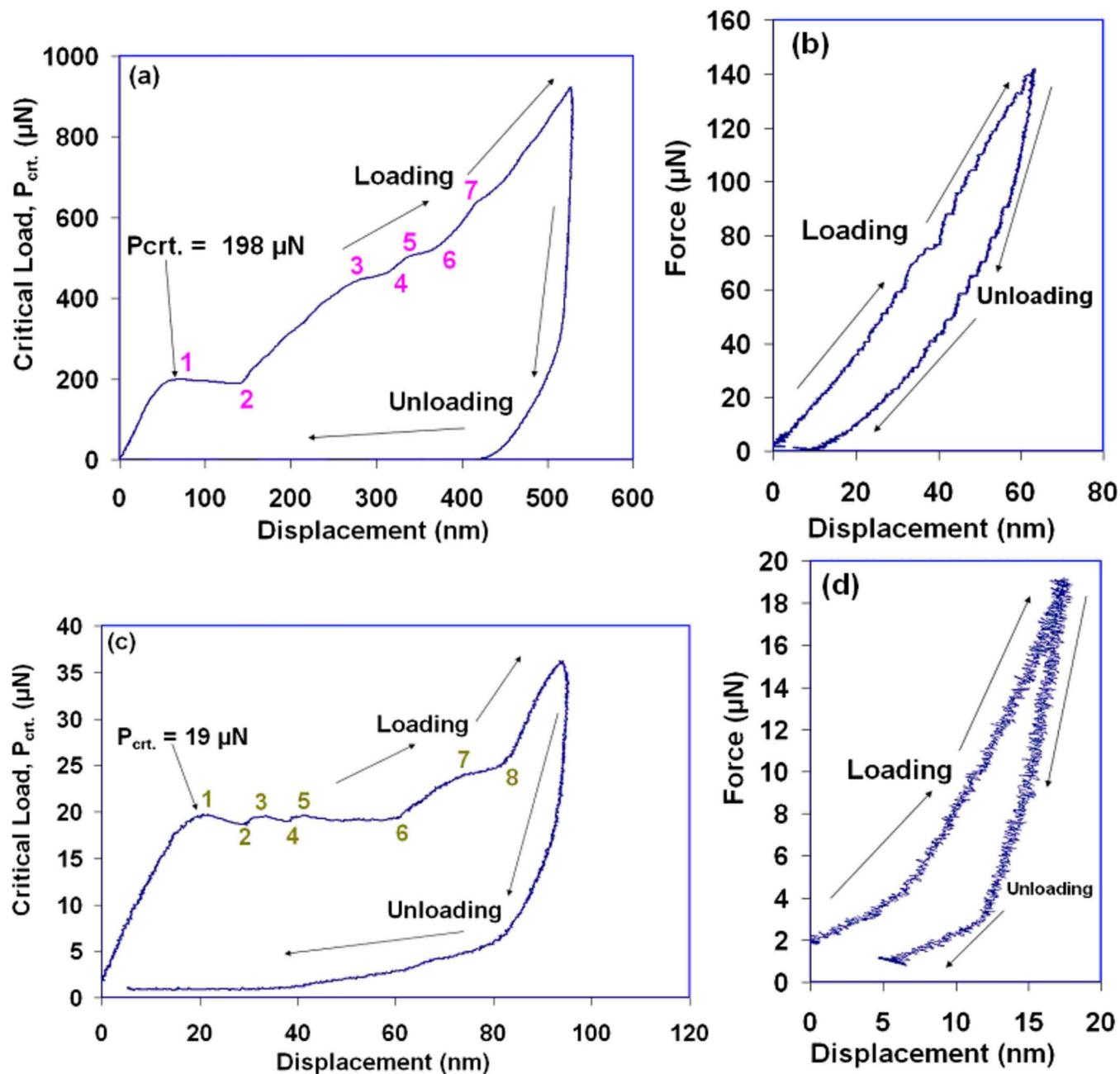
FIG. 3. (Color online) Load vs displacement curve of the as-grown ZnO nanorods/nanowires from nanoindentation experiments, where (a) and (c) show load displacement curves for kinking and buckling, and (b) and (d) show the bending flexibility curves for the ZnO nanorods/nanowires grown by the VLS method on the SiC and Si substrates.

proximately linear up to the first critical point during both the bending and buckling tests. This elastic linearity may be due to their low dimensionality and single crystallinity, which provides few defects and a low dislocation moment in the material. As their stacking fault energy is low, the II-VI semiconductors then tend to have a large density of twins and stacking faults.[26] The critical resolved shear stress for plastic deformation is low and dislocations are easily created.[27] Our results reflect that the as-grown ZnO nanorods/nanowires were elastic, single crystal, and good quality.

Figures 2(a), 2(c), 3(a), and 3(c) also show that a displacement, deflection, or bending of the nanorods/nanowires has multiple kinks and inflection points. This shows that after the first critical point, the nanorod/nanowires have some plasticity due to the moment of dislocations. This is because ZnO belongs to the II-VI semiconductors, and due to the factors mentioned above,[26,27] dislocations and plasticity can easily be created. Up to the first critical point, loading and deflection have a very good linear relationship, showing that our as-grown nanorods/nanowires are elastic and flexible. This elasticity and flexibility is due to the low dimensionality of the structure. Chen *et al.*[9] showed that a pure single ZnO crystal of 100 nm diameter can be bent into a circle of one micrometer minimum diameter. Another cause of the elasticity and flexibility may be the movement of the nanorods of the support at the ends, as a perfect rigid support is impossible. Also, in slender columns or shells, the membrane stiff-
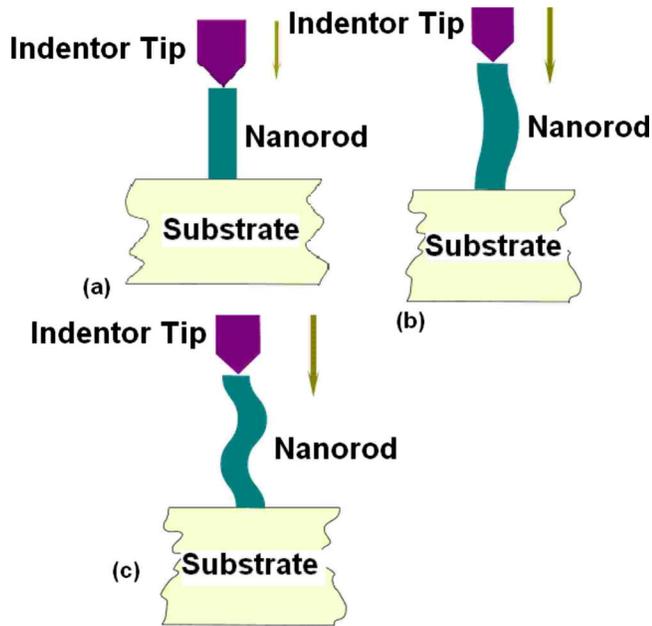
FIG. 4. (Color online) Shows different stability conditions: (a) stable, (b) critically stable, and (c) unstable.

ness is much greater than the bending stiffness, and a large membrane strain can be stored with small deformation, so when buckling occurs, comparatively large bending deformations are needed to absorb the membrane strain energy released.[25] This can be seen in Tables I–IV, where the strain energies for a single nanorod/nanowire of the as-grown samples were calculated and are much smaller than the corresponding calculated buckling energies. This shows that our as-grown ZnO nanorods/nanowires are flexible. Such an experiment is of great interest for piezoelectric nanodevices.

The behavior of an ideal column under an axial compressive load can be summarized as will be described as follows.[13] If the load, P is less than the critical load P_{crt}, the nanorods or columns are in stable equilibrium. In Figs. 2(a), 2(b), 3(a), and 3(b), zone 0-1 of the loading portion falls under this condition. This is also described in Fig. 4(a). If the load P is equal to the critical load P_{crt}, the nanorods or columns are in neutral equilibrium. In Figs. 2(a), 2(c), 3(a), and 3(c) zone 1-2 of the loading portion falls under this condition, as is also shown in Fig. 4(b). If the load P is greater than the critical load P_{crt}, the nanorods or columns are either in unstable equilibrium or an alternative buckled configuration develops. In Figs. 2(a) and 2(c) and 3(a) and 3(c) zones

TABLE I. Slenderness ratio, critical, or buckling stress, buckling strain, Buckling energy, $E_b = 3.15 \times 10^{-12}$ J, strain energy, and modulus of elasticity for single crystal vertical ZnO nanorods grown on SiC substrates by the ACG method (bulk crystal of ZnO modulus of elasticity, $E = 140.0$ GPa, yield strength $S_y = 7.0$ GPa) (Refs. 9 and 18).

End condition of nanorods	C	$(l/k)_{P'}$	$(l/k)_{actual'}$	Strain energy $\times 10^{-15}$ (J)	Experimental critical stress σ_c (MPa)	Modulus of elasticity E (GPa)	Critical strain ε_c (%)	Analysis model
Fixed-free	0.25	9.93	57.50	0.563	77.40	103.70	0.0746	Euler
Pinned-pinned	1.00	20.0	57.50	2.25	77.40	25.925	0.2985	Euler
Fixed-pinned	2.00	28.1	57.50	4.5	77.40	12.96	0.597	Euler
Fixed-fixed	4.00	40.0	57.50	9.0	77.40	6.48	1.194	Euler

TABLE II. Slenderness ratio, critical or buckling stress, buckling strain, buckling energy, $E_b = 2.337 \times 10^{-12}$ J, strain energy and modulus of elasticity for single crystal vertical ZnO nanorods grown on Si substrates by the ACG method (bulk crystal of ZnO modulus of elasticity, $E = 140.0$ GPa, yield strength $S_y = 7.0$ GPa) (Refs. 9 and 18).

End condition of nanorods	C	$(l/k)_{P'}$	$(l/k)_{actual'}$	Strain energy $\times 10^{-15}$ (J)	Experimental critical stress σ_c (MPa)	Modulus of elasticity E (GPa)	Critical strain ε_c (%)	Analysis model
Fixed-free	0.25	9.93	13.43	0.025	221.3	16.2	0.013 66	Euler
Pinned-pinned	1.00	20.0	13.43	1.23	221.3	33.0	0.67	J.B. Johnson
Fixed-pinned	2.00	28.1	13.43	2.45	221.3	16.5	1.34	J.B. Johnson
Fixed-fixed	4.00	40.0	13.43	4.90	221.3	8.25	2.68	J.B. Johnson

TABLE III. Slenderness ratio, critical or buckling stress, buckling strain, buckling energy, $E_b = 7.03 \times 10^{-12}$ J, strain energy, and modulus of elasticity for single crystal vertical ZnO nanorods grown on the SiC substrate by the VLS method (bulk crystal of ZnO modulus of elasticity, $E = 140.0$ GPa, yield strength $S_y = 7.0$ GPa) (Refs. 9 and 18).

End condition of nanorods	C	$(l/k)_{P'}$	$(l/k)_{actual'}$	Strain energy $\times 10^{-14}$ (J)	Experimental critical stress σ_c (MPa)	Modulus of elasticity E (GPa)	Critical strain ε_c (%)	Analysis model
Fixed-free	0.25	9.93	22.03	5.40	162.83	32.03	0.508	Euler
Pinned-pinned	1.00	20.0	22.03	21.54	162.83	8.0	2.032	Euler
Fixed-pinned	2.00	28.1	22.03	3.92	162.83	44.07	0.37	J.B. Johnson
Fixed-fixed	4.00	40.0	22.03	7.84	162.83	22.035	0.74	J.B. Johnson

TABLE IV. Slenderness ratio, critical or buckling stress, buckling strain, buckling energy, $E_b = 1.805 \times 10^{-13}$ J, strain energy, and modulus of elasticity for single crystal vertical ZnO nanorods grown on the Si substrate by the VLS method (bulk crystal of ZnO modulus of elasticity, $E = 140.0$ GPa, yield strength $S_y = 7.0$ GPa) (Refs. 9 and 18).

End condition of nanorods	C	$(l/k)_{P'}$	$(l/k)_{actual'}$	Strain energy $\times 10^{-16}$ (J)	Experimental critical stress σ_c (MPa)	Modulus of elasticity E (GPa)	Critical strain ε_c (%)	Analysis model
Fixed-free	0.25	9.93	54.64	0.0283	51.0	61.71	0.083	Euler
Pinned-pinned	1.00	20.0	54.64	1.133	51.0	15.43	0.332	Euler
Fixed-pinned	2.00	28.1	54.64	2.266	51.0	7.714	0.664	Euler
Fixed-fixed	4.00	40.0	54.64	4.532	51.0	3.86	1.328	Euler

2-3, 3-4, 4-5, 5-6, 6-7, and 7-8 of the loading portion fall under this condition, as is also shown in Fig. 4(c). The general form of the Euler equations for long vertical nanorods/nanowires and the J.B. Johnson equation for intermediate nanorods/nanowire, and the corresponding analysis, can be found in Refs. 13 and 22.

We can also calculate the average buckling load of an individual ZnO nanorod/nanowire. The diamond tip that we were using is of conical shape (60° solid angle) and is 1 μm in radius. Therefore, approximately 120 and 90 nanorods/nanowires grown by the ACG method were loaded axially on the SiC and Si substrates used in this study, respectively, and thus, the average buckling load of an individual nanorod is approximately 0.875 μN on the SiC substrate and 1.27 μN on the Si substrate. Similarly approximately 16 and 189 nanorods were loaded axially on the samples grown by the VLS method, such that the average bucklings or critical loads bear by a single nanorod/nanowire are approximately 12.375 and 0.10 μN, respectively, for the SiC and Si substrates. These critical loads born by a single nanorod are used to deduce the modulus of elasticity, critical stress, strain, and the strain energy in the individual nanorod/nanowire.

In Figs. 2(a), 2(c), 3(a), and 3(c), and considering zone 0-1 in which the load is almost linear up to the first critical point, in this region we assume that the linear elasticity theory is applicable. According to the linear elasticity theory, the stress is directly proportional to the strain,

$$\sigma_c = E\varepsilon_c, \tag{1}$$

$$\sigma_c = \frac{P_{crt}}{A}, \tag{2}$$

$$U = \frac{1}{2}\sigma\varepsilon_c V, \tag{3}$$

where σ_c, ε_c, U, and V are the critical stress, critical strain, strain energy, and volume of the single nanorod/nanowire.

As ZnO is ceramic and behaves as an inductile material, the compressive strength is equal to the yield strength. For bulk ZnO we use the modulus of elasticity $E = 140$ GPa (Ref. 9) and yield strength $S_y = 7.0$ GPa.[18] Using the classification of nanorods/nanowires as long, intermediate, end conditions, and the analysis models in Refs. 13 and 22 the modulus of elasticity, critical stress, critical strain, and strain energy are calculated and are given in Tables I–IV, respectively.

As shown in Tables I–IV, we determined the modulus of elasticity (E) of the ZnO nanorods and its corresponding buckling stress (σ_c), critical strain (ε_c), and strain energy for different end conditions of the nanorods. It should be noted that the contributions of the end condition and the slenderness ratio put the analysis within both the Euler and J.B. Johnson models. As we used the average values of length and diameter, the calculated values in the given tables may have some deviation from the true values. The values of the modulus of elasticity, E for the as-grown ZnO nanorods/nanowires grown by ACG method on SiC and Si substrates are about 6–104 and 8–33 GPa, respectively. Similarly, for the as-grown sample by the VLS method, the approximate ranges of modulus of elasticity for the single rod/wire are 8–44 and 4–62 GPa, respectively. It should be noted that the value of Young's modulus of elasticity of the single crystal ZnO nanorods grown on SiC substrates by ACG and on Si substrates by the VLS method have higher values because of the larger slenderness ratio compared to the other samples. This reveals that buckling is a structural rather than material property. In this report, we investigated by applying classical way of bending flexibility, kinking, and buckling characterization of vertical single crystal ZnO nanorods/nanowires oriented along the c-axis on different substrates by a hysitron nanoindenter. Our experimental first buckling critical point and the highest bending point were very similar, which shows that our nanorods/nanowires are elastic and then become brittle after ceasing of the prebuckled configuration due to the plasticity effect. Based on the Euler buckling model and the J.B. Johnson parabolic model, we found that the value of E decreases with decreasing of the slenderness ratio and vice versa as compared to Refs. 19 and 20. Since buckling is a structural rather than a material failure mechanism, there is no microstructure consideration and analytic methods are based on the principle of elasticity and continuum mechanics.

IV. CONCLUSION

In this research work, the main focus was the experimental observation and characterization of the bending flexibility, kinking and buckling failure phenomena of well-aligned single crystal ZnO nanorods/nanowires. These nanostructures were grown by the ACG method, a relatively low temperature approach, and by the VLS method, which is a relatively high temperature approach, on SiC and Si substrates. The first inflection, kink, and critical point of the as-grown

ZnO nanorods/nanowires are found to be 105, 114, 198, and 19 μN, respectively. The corresponding buckling energies were also calculated are 3.15×10^{-12}, 2.337×10^{-12}, 7.03×10^{-12}, and 1.805×10^{-13} J, respectively. Bending flexibility characterization shows that the loading and unloading behaviors of the as-grown ZnO nanorods/nanowires are highly symmetrical. The first inflection or critical buckling point and the corresponding highest bending point in all the curves for all the samples are very close. This shows that our as-grown nanorods/nanowires have linear elastic behavior in the vertical configuration. We found that the ACG as-grown nanorods on the SiC substrates and the VLS grown ones on the Si substrates have highest modulus of elasticity and lowest critical buckling point. This is due to the larger slenderness ratio as compared with the other samples. The buckling energies calculated from the experiments were also calculated and found to be much greater than the strain energy of the as-grown samples. This also shows that our as-grown nanorods/nanowires are well aligned along the *c*-axis on the substrates. We have used the Euler model for long nanorods and the J.B. Johnson model for intermediate nanorods for the evaluation of the modulus of elasticity, critical stress, critical strain, and strain energy of single ZnO nanorod for each sample. It was observed that the modulus of elasticity (E) is dependent on the slenderness ratio and independent of the growth method. We concluded that the kinking and buckling failure is a design or structure failure rather than a material failure, and also observed that the buckling is independent of the growth method. It is strongly dependent on the verticality and the surface properties of the substrates. We also concluded that ZnO nanorods/nanowires show flexibility and plasticity after the first critical point. Due to this plasticity, multiple kinks were observed.

[1] Y. Qin, X. Wang, and Z. L. Wang, Nature (London) **451**, 809 (2008).

[2] X. Duan, Y. Huang, Y. Cui, J. Wang, and C. M. Lieber, Nature (London) **409**, 66 (2001).

[3] M. H. Huang, S. Mao, H. Feick, H. Yan, Y. Wu, H. Kind, E. Weber, R. Russo, and P. Yang, Science **292**, 1897 (2001).

[4] M. Willander, Y. E. Lozovik, Q. X. Zhao, O. Nur, Q. H. Hu, and P. Klason, Proc. SPIE **6486**, 648614 (2007).

[5] S. Al-Hilli, A. Öst, P. Strålfors, and M. Willander, J. Appl. Phys. **102**, 084304 (2007).

[6] X. D. Bai, P. X. Gao, Z. L. Wang, and E. G. Wang, Appl. Phys. Lett. **82**, 4806 (2003).

[7] Z. L. Wang and J. H. Song, Science **312**, 242 (2006).

[8] Q. X. Zhao, P. Klason, M. Willander, P. J. Bergman, W. L. Jiang, and J. H. Yang, Phys. Scr. **T126**, 131 (2006); H. Zhou, M. Wissinger, J. Fallert, R. Hauschild, F. Stelzl, C. Klingshirn, and H. Kalt, Appl. Phys. Lett. **91**, 181112 (2007).

[9] C. Q. Chen, Y. Shi, Y. S. Zhang, J. Zhu, and Y. J. Yan, Phys. Rev. Lett. **96**, 075505 (2006).

[10] S. Muthukumar, H. Shen, J. Zhong, Z. Zhang, N. W. Emantoglu, and Y. Lu, IEEE Trans. Nanotechnol. **2**, 50 (2003).

[11] D. C. Look, Mater. Sci. Eng., B **80**, 383 (2001).

[12] P. X. Gao and Z. L. Wang, J. Appl. Phys. **97**, 044304 (2005).

[13] J. E. Shigley, C. R. Mischke, and R. G. Budynas, *Mechanical Engineering Design*, 7th ed. (McGraw-Hill, New York, 2004).

[14] G. Feng, W. D. Nix, Y. Yoon, and C. J. Lee, J. Appl. Phys. **99**, 074304 (2006).

[15] A. V. Desai and M. A. Haque, Sens. Actuators, A **134**, 169 (2007).

[16] J. Song, X. Wang, E. Riedo, and Z. L. Wang, Nano Lett. **5**, 1954 (2005).

[17] M. Lucas, W. Mai, R. Yang, Z. L. Wang, and E. Riedo, Nano Lett. **7**, 1314 (2007).

[18] C. Q. Chen and J. Zhu, Appl. Phys. Lett. **90**, 043105 (2007).

[19] S. J. Young, L. H. Ji, S. J. Chang, T. H. Fang, T. J. Hsueh, T. H. Meen, and I. C. Chen, Nanotechnology **18**, 225603 (2007).

[20] L. W. Ji, S. J. Young, T.H. Fang, and C. H. Liu, Appl. Phys. Lett. **90**, 033109 (2007).

[21] S. O. Kucheyev, J. E. Bradby, J. S. Williams, C. Jagadish, and M. V. Swain, Appl. Phys. Lett. **80**, 956 (2002).

[22] M. Riaz, O. Nur, M. Willander, and P. Klason, Appl. Phys. Lett. **92**, 103118 (2008); **92**, 179902(E) (2008).

[23] M. Riaz, A. Fulati, Q. X. Zhao, O. Nur, P. Klason, and M. Willander, Nanotechnology **19**, 415708 (2008).

[24] L. Greene, M. Law, D. Tan, M. Montano, J. Goldberger, G. Somorjai, and P. Yang, Nano Lett. **5**, 1231 (2005).

[25] R. D. Cook, D. S. Malkus, M. E. Plesha, and R. J. Witt, *Concepts and Application of Finite Element Analysis*, 4th ed. (Wiley, Hoboken, NJ, 2002).

[26] S. Jain, M. Willander, and V. Overstraeten, *Compound Semiconductors Strained Layers and Devices*, Electronic Materials 7 (Kluwer Academic, Norwell, MA, 2000).

[27] T. Asahi, O. Oda, and Y. Koyama, J. Cryst. Growth **161**, 20 (1996).